# Kinetic and Mechanistic Modeling of Acid-Catalyzed Degradation of Polymers with Various Cracking Catalysts

**Yeuh-Hui Lin, Mu-Hoe Yang**

*Department of Chemical and Biochemical Engineering, Kao Yuan University, Kaohsiung, Taiwan, Republic of China*

Received 17 October 2008; accepted 5 April 2009
DOI 10.1002/app.30787
Published online 7 July 2009 in Wiley InterScience (www.interscience.wiley.com).

**ABSTRACT:** A new approach is presented that combines kinetic and mechanistic considerations which take into account chemical reactions and catalyst deactivation in the modeling of the catalytic degradation of polymers. Though acid-catalyzed hydrocarbon cracking reactions involve a large number of compounds, reactions and catalyst deactivation and are very complex, the model gives a good representation of experimental results from the degradation of polyethylene and polypropylene over fluidized acidic catalysts. This model provides the benefits of product selectivity for the chemical composition such as alkanes, alkenes, aromatics, and coke in relation to the effect of structurally different polymer feeds, the performance of the catalyst and the selection of their particle sizes, and the influence of different reaction temperatures. It is an improvement of the currently available empirical "lumping" techniques which usually are severely restricted in terms of product definitions. © 2009 Wiley Periodicals, Inc. J Appl Polym Sci 114: 2591–2599, 2009

**Key words:** catalytic degradation; polymers; cracking catalysts; kinetics; modeling

## INTRODUCTION

Polymer waste can be regarded as a potential source of chemicals and energy. Methods for recycling polymer waste have been developed and new recycling approaches are being investigated.[1] Chemical recycling, i.e., conversion of waste polymers into feedstock or fuels, has been recognised as an ideal approach and could significantly reduce the net cost of disposal.[2] Several reports[3–7] described the conversion of polymer waste by noncatalytic thermal degradation. Other reports address the role of acid catalysts in the catalytic degradation of polymers.[8–13] Although the result of these studies has been the improvement of the catalyst, there is still a need to develop kinetic models to describe the experimental results and to facilitate the further development of a process to industrial scale.

Articles concerning kinetic modeling of catalytic process for polymer degradation have great limitations, which are shared with the study of other complex reaction schemes such as catalytic cracking and reforming. The kinetic models proposed in the literature can be grouped into (i) kinetic models based on thermal analysis of the weight loss curves,[14–16] (ii) kinetic models based on reaction mechanism and elementary steps[17–19] and (iii) models with lumping schemes.[20–23] In the case of thermal analysis, the shortcoming is in general excessive simplification either in the assumed kinetic scheme or in the handing of experimental data. Kinetic models with individual reaction steps lead to a great number of kinetic parameters, whose application for the simulation of industrial reactors is difficult. In the lumped kinetic models, the large number of individual constituents in a complex feedstock can be grouped into the broad but measurable categories of compound classes, with simplified reaction networks between the lumps. These lumped models may be useful for the needs of reactor design, but there still exist some inherent limitations. Firstly, the approach often fails to extrapolate to different feedstock because of composition differences within the same defined lumps. Secondly, coarsely lumped models cannot be utilized to interpret the effects of catalyst properties on the phenomenological aspects of catalytic properties because fundamental catalytic reaction mechanisms are not incorporated into the kinetic scheme. Thirdly, insufficient detail exists in the lumped models to predict subtle changes in product properties.

Mechanistic considerations of catalytic degradation of hydrocarbons have largely been focused on small molecules ($<C_{16}$) rather than on macromolecules such as polymers. The literature available involving the mechanistic considerations for catalytic

*Correspondence to:* Y.-H. Lin (lin@cc.kyu.edu.tw).
Contract grant sponsor: National Science Council (NSC) [Republic of China (ROC)]; contract grant number: NSC 95-2211-E-244-013.

**TABLE I**
**Properties of Various Cracking Catalysts Used in the Catalytic Degradation of Polymer**

| Catalyst | Si/Al | Acidity[a] (μ mol Py/g catalyst) | | Surface area ($m^2/g$) | | | Pore size (nm) | Commercial name |
|---|---|---|---|---|---|---|---|---|
| | | Brψnsted | Lewis | BET | Micropore | External | | |
| HZSM-5 | 17.5 | 22.4 | 13.8 | 426 | 263 | 128 | 0.55 × 0.51 | ZSM-5 zeolite[b] |
| ECat-1 | 2.1 | 6.3 | 3.9 | 386 | 295 | 91 | –[c] | Equilibrium catalysts[b] |
| SAHA | 2.6 | 2.8 | 21.8 | 268 | 21 | 247 | 3.28[d] | Amorphous silica alumina[e] |

[a] Acidity of catalysts as measured by IR-pyridine experiments at 300°C.
[b] Chinese Petroleum Corp., CPC, Taiwan, ROC.
[c] The catalyst was a mixture of zeolite with 1.3 wt % rare earth oxide (REO), a silica-alumina. matrix (32.5 wt % $Al_2O_3$) and binder.
[d] Single-point BET determined.
[e] Crosfield Chemicals, Warrington, UK.

polymer degradation is rather scarce. Potential concepts have been investigated in our group using a laboratory catalytic fluidized bed reactor to study the product distribution and selectivity of catalytic degradation of postconsumer polymer wastes previously.[24,25] In these studies, the catalysts increase significantly the commercial potential of a recycling process based on catalytic degradation, as cracking catalysts could cope with the conversion of plastic waste cofed into a refinery fluidizing catalytic cracking (FCC) unit. Therefore, a more interesting approach is that of adding polymer waste into the FCC process, under suitable process conditions with the use of zero value of spent FCC catalysts, a large number of polymers can be economically converted into valuable hydrocarbons. Additionally, our study[26] has used thermogravimetric analysis (TGA) as a potential method for screening catalysts in the catalytic degradation of polypropylene (PP). The objective of this work is to use a kinetic/mechanistic model to study the production rates and product selectivity on the catalytic reactions of different polymers with spent FCC catalysts (ECat-1) and various cracking catalysts, and provide some basis to enhance the potential benefit of catalytic polymer recycling.

## EXPERIMENTAL

### Materials and experimental procedures

The polymers used in the experiment were pure polyethylene (PE; unstablized, $M_w \approx 93{,}000$, $\rho = 960.3$ $kgm^{-3}$, BASF) and pure polypropylene (PP; isotactic, $M_w \approx 330{,}000$, $\rho = 851.6$ $kgm^{-3}$, Aldrich). Both PE and PP were pyrolysed over zeolites (HZSM-5), equilibrium spent FCC catalysts (ECat-1) and a Silica-alumina (SAHA) catalyst under identical reaction conditions. The catalysts employed and their preparations are given elsewhere[24] and described in Table I. All the catalysts were pelleted, crushed, and sieved to give particle sizes ranging from 75 to 180 μm. The structural and textural differences with their acidic properties are also given in Table I. The acid strength of the catalysts was measured by IR spectroscopy and adsorption–desorption of pyridine (Py). By using the value of the integrated molar extinction coefficients for the band at 1545 $cm^{-1}$ (Py adsorbed on Brψnsted acid sites) and for the band at 1450 $cm^{-1}$ (Py adsorbed on Lewis acid sites), the amount of adsorbed Py (μmol/g) on both acid sites of catalysts can be obtained. Surface area, pore volume and pore size distribution were measured from the adsorption–desorption isotherms of nitrogen at 77 K. Pore size distribution was obtained following the BJH model, whereas the micropore specific surface area and the micropore volume were calculated by the t-plot method. The fresh catalyst was then dried by heating in flowing nitrogen (50 mL $min^{-1}$) to 120°C at 60°C $h^{-1}$. After 2 h the temperature was increased to 520°C at a rate of 120°C $h^{-1}$ to active the catalyst for 5 h. In the case of the equilibrium spent FCC catalyst (ECat-1), it could contain a certain amount of coke, and air was swept and maintained for 3 h at 600°C to burn it off before activating.

The particle size of both catalyst (75–120 μm) and polymer (75–250 μm) was chosen as being large enough to avoid entrainment. The catalyst was small enough to be adequately fluidized. Due to at the different operating conditions was calculated, Since the velocities in the range 1.5–4 times the value of the minimum fluidation velocity ($U_{mf}$) of catalyst were used in the course of this work, the catalyst particles move freely. On addition the polymer, the fluidized bed remains fluidized at sufficiently low polymer/catalyst ratios used in this study. A detailed description of the experimental system was given elsewhere.[25] Gaseous products were analyzed using a gas chromatograph equipped with a thermal conductivity detector and a flame ionization detector. The solid remaining deposited on the catalyst after the catalytic degradation of the polymer were deemed "residues" and contained involatile

**TABLE II**
**Product Distributions of PE and PP Degradation at Reaction Temperature of 360°C Over Various Catalysts**

| | HZSM-5 | | ECat-1 | | SAHA | |
|---|---|---|---|---|---|---|
| Yield (wt % feed) | PE | PP | PE | PP | PE | PP |
| Gases (C1–C4) | 64.1 | 67.5 | 40.8 | 39.1 | 30.3 | 22.5 |
| Gasoline(C5–C9) | 27.1 | 25.1 | 47.7 | 50.4 | 54.2 | 63.5 |
| Liquid | 2.3 | 2.3 | 3.2 | 3.5 | 3.4 | 4.4 |
| Residue | 4.3 | 3.5 | 7.2 | 6.3 | 12.1 | 9.4 |
| Involatile | 2.8 | 2.6 | 3.1 | 2.4 | 9.6 | 7.6 |
| Coke | 1.7 | 1.1 | 3.9 | 3.7 | 2.5 | 1.8 |
| BTX | 2.2 | 1.7 | 1.1 | 0.8 | – | – |
| $C_4$ and $C_5$ hydrocarbons | | | | | | |
| i-$C_4H_{10}$ | 8.4 | 10.6 | 13.2 | 11.8 | 1.6 | 0.7 |
| n-$C_4H_{10}$ | 1.8 | 2.1 | 0.7 | 0.3 | 0.1 | n.d |
| $C_4H_8$ | 26.7 | 24.7 | 11.3 | 16.6 | 20.9 | 17.9 |
| i-$C_5H_{12}$ | 4.3 | 4.5 | 14.2 | 10.9 | 1.0 | 0.4 |
| n-$C_5H_{12}$ | 0.7 | 0.7 | 0.3 | – | n.d | n.d |
| $C_5H_{10}$ | 12.5 | 11.6 | 7.5 | 14.7 | 23.3 | 21.4 |

Catalyst particle size = 75–120 μm, fluidizing $N_2$ rate = 570 mL $min^{-1}$ and polymer to catalyst ratio = 40% wt/wt.

Liquid: condensate in condenser and captured in filter; Residue: coke and unconverted polymer; BTX: benzene, toluene and xylene; – : less than 0.01%; n.d.: not detectable.

products and coke. Mass balances were, in most cases, greater than 95%. The amount and nature of the residues was determined by TGA.

### Experimental results

For simplicity, catalytic pyrolysis products are grouped together as hydrocarbon gases (<$C_5$), gasoline up to $C_9$ ($C_5$–$C_9$), liquids (condensate in condenser and filter) and residues (coke and products, involatile at reaction temperature, deposited on catalyst) to enable the overall pyrolysis processes to be described more easily. Table II summarizes the products of PE and PP degradation over various catalysts. The bulk of the products observed were in the gas phase (>85 wt %) with less than 5 wt % liquid collected. The highest level of unconverted polymer was observed with SAHA, whilst the highest coke yield was observed with ECat-1. HZSM-5 yielded the amount of $C_1$-$C_4$ and $C_5$-$C_9$ products, which were ~ 68 wt % and 25 wt % respectively with the highest level of BTX. However, ECat-1 gave the different $C_1$-$C_4$ and $C_5$-$C_9$ yields, which was ~ 35 wt % and 54 wt % respectively with about 13 wt % of an iso-$C_4$ paraffin.

## THE MODEL

### Kinetic and mechanistic aspects

SEM studies previously[27] using a heated stage indicate that, for premixed polymer/catalyst particles, at temperatures around 300°C, the molten polymer is drawn into the spaces between particles and hence to active sites at the external surface of zeolite catalysts or in larger pores of amorphous materials. Surface reaction then produces lower molecular weight materials which, if sufficiently volatile at reaction temperature, can either diffuse through the polymer film, as products, or react further in the pores, including micropores, of zeolites. As a result, product distributions reflect features of the zeolite catalysts in relation to their pore systems and chemical composition. This is evident in the product distributions shown in Table II. For example, comparison of HZSM-5 and ECat-1 in cracking PP shows the expected increase in bimolecular hydrogen transfer typical of the large ring, large cavity, Y structure versus the medium pore HZSM-5. This is reflected in the alkane/alkene ratios in the $C_4$ and $C_5$ products. In fact the pattern of the $C_4$ alkanes and alkenes is very similar to that observed in gas oil and gasoline cracking[28] and results can be explained in a similar manner.

A general mechanistic reaction scheme involving the discussion of the carbenium ion of catalytic cracking chemistry for the degradation of hydrocarbon has been proposed.[29] This representation is simplified regarding the formation of carbenium ions in that it concentrates on reaction paths rather than on surface species. Theoretical studies suggest that, for the conversion of hydrocarbons on active zeolites, reactions proceed via carbenium ions as transition states (rather than as intermediates) and product distributions are also generally in agreement with

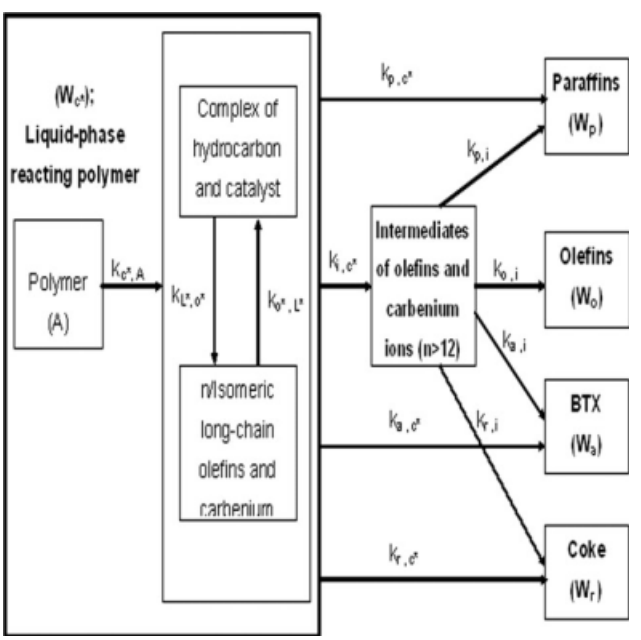


**Figure 1** A mechanistic and kinetic scheme representing polymer degradation over cracking catalysts.

carbenium ion studies, although there is still debate about the actual mode of scission.[30] In this article, a kinetic/mechanistic model including the main mechanistic features and kinetic reaction schemes for polymer degradation over cracking catalysts is investigated (Fig. 1). The added polymer mixture melts, wets the catalyst surface and is pulled into the catalyst macropores by capillary action.[24] The polymer coating the particles is stated to be liquid, and for the reactions that occur on the interior pore surface the situation would seem to be completed. Initially, solid polymer is freely dropped into the reactor and immediately melts to disperse around the catalysts. The molten polymer, in contact with the catalyst particle forms a polymer/catalyst complex, reaction commencing at the surface. Gaseous products are forced out to have diffused and produced on the interior surface. The model uses the following assumptions.

1. The liquid-phase polymer. Initially, solid polymer is freely dropped into the reactor and immediately melts to disperse around the catalysts. The molten polymer, in contact with the catalyst particle forms a polymer/catalyst complex, reaction commencing at the surface.
2. Evolution of intermediates. Scission reactions generate intermediates which include long-chain olefins and intermediate precursors for carbenium ions. The carbenium ions rapidly reach a steady-state concentration. Alkanes may be generated, via hydrogen transfer, and initially will be largely long-chain products. In general, the number of active sites limits the number of carbenium ion precursors.
3. Evolution of products. Once the intermediates are produced, further reactions could be expected to produce smaller chain olefins in equilibrium with surface carbenium ions, as well as alkanes, BTX (Benezene, Toluene and Xylene) and coke. The equilibrium mixture of olefins and carbenium ions subsequently reacts further to produce the final products.

### The reaction scheme and rate expressions

On the basis of the reaction pathway shown in Figure 1, the rate of formation, $r_{i,j}$, of the product $i$ from reactant $r$, through reaction $j$ can be written as

$$r_{i,j} = k_{i,j} \times W_r^{n_j} \times \eta_j \quad (1)$$

where $r_{i,j}$ is the rate constant of the product $i$ from the $j$th reaction, $W_r$ is the weight fraction of the reactant $r$ present on the acid sites, $\eta_j$ is the catalyst activity decay of the $j$th reaction, $n_j$ is the reaction order of the $j$th reaction. An exponential decay function with activity decaying as function of coke on catalyst was employed for PP on ECat-1.

$$\eta = \exp[-\alpha \times C(c)] \quad (2)$$

where $C(c)$ is coke content deposited on the catalyst and $\alpha$ is a constant for PP.[26] For the model we consider, as an approximation, that $\alpha$, in the deactivation process, can be taken as constant for both polymers and that the active sites are deactivated at the same rate for the acid catalysts studied. The activity decay, $\eta_j$, was assumed to be the same for all reaction steps with the activity proportional to the number of remaining sites.

$$\eta_j = \eta = \exp(-\alpha \times W_r) \quad (3)$$

where $W_r$ is coke content deposited on the individual catalyst. Equations (4)–(9) were obtained assuming that reaction rates can be represented by simple first-order processes (i.e. $n_j = 1$) and catalyst deactivation involving six simultaneous equations. Polymer cracking is known to proceed over acidic catalysts by carbocation mechanisms, where the initially formed ions undergo chain reactions via processes, such as scission or β-scission and isomerization and hydrogen-transfer alkylation and oligomerization, to yield typically smaller cracked products. For PP degradation over a spent FCC catalyst, an exponential decay function with activity decaying as function of coke on catalyst with the apparent reaction order of 1 was reported previously.[26] The mechanism involved is associated with the diffusion of bulky fragments for the unreacted or partially reacted polymer softened by dissolution of low molecular species deposited on the catalyst. Thus, the effect of coke produced during the course of the reaction was to obstruct active sites, and that the uncovered sites would give rise to the same reaction mechanism, and also can therefore give the same apparent reaction order in this study. Initially, surface reaction forms a complex of molten polymer/catalyst. Thus, the rate of the consumption of the lumped liquid-phase polymer species ($W_{c^*}$) can be written as.

$$-dW_{c^*}/dt = \eta \times (k_{i,c^*} + k_{p,c^*} + k_{a,c^*} + k_{r,c^*}) \times W_{c^*} \quad (4)$$

Therefore, the formation of intermediates of olefins and carbenium ions ($n > 12$) can be expressed as

$$dW_i/dt = \eta \times [(k_{i,c^*} \times W_{c^*}) - (k_{o,i} + k_{p,i} + k_{a,i} + k_{r,i}) \times (W_i)] \quad (5)$$

Similarly, the evolution of the olefinic lump ($W_o$), the paraffinic lump ($W_p$), the BTX lump ($W_a$), and the coke lump ($W_r$) are described as follows:

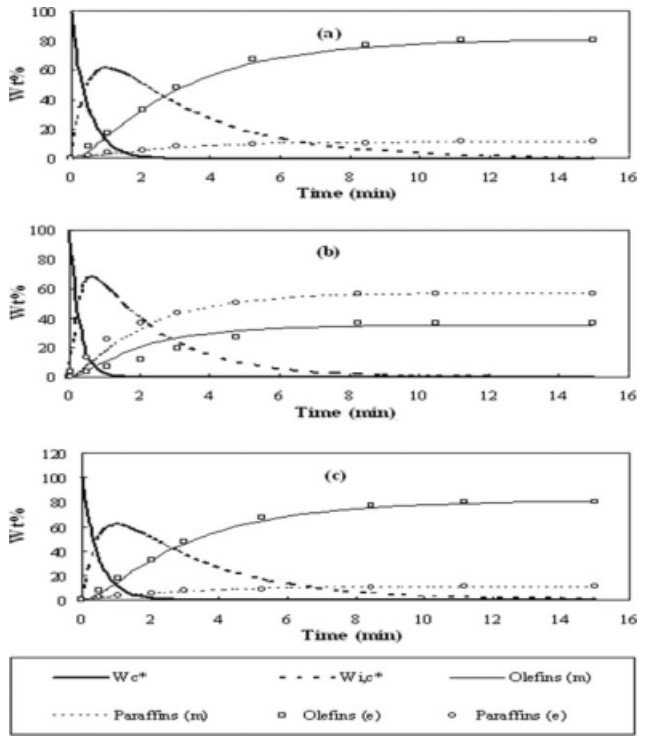


**Figure 2** Comparison of calculated (m) and experimental (e) results some main products for the degradation of PP over (a) HZSM-5, (b) ECat-1 and (c) SAHA catalysts at 360°C (catalyst particle size = 75–120 μm, fluidizing $N_2$ rate = 570 mL $min^{-1}$ and polymer to catalyst ratio = 40% wt/wt).

$$dW_o/dt = \eta \times k_{o,i} \times W_i \quad (6)$$

$$dW_p/dt = \eta \times [k_{p,i} \times (W_i) + (k_{p,c^*} \times W_{c^*})] \quad (7)$$

$$dW_a/dt = \eta \times [k_{a,i} \times (W_i) + (k_{a,c^*} \times W_{c^*})] \quad (8)$$

$$dW_r/dt = \eta \times [k_{r,i} \times (W_i) + (k_{r,c^*} \times W_{c^*})] \quad (9)$$

The mass balance can be written as

$$-dW_{c^*}/dt = dW_i/dt + dW_o/dt + dW_p/dt + dW_a/dt + dW_r/dt \quad (10)$$

Equations (4)–(10) were numerically integrated by a fourth-order Runge-Kutta algorithm with Matlab to very the individual rate constants by minimizing the sum of the squared deviations between calculated and experimental results. This gave values for the apparent rate constants.

## RESULTS AND DISCUSSION

The kinetic/mechanistic model has been used to represent product distributions for the degradation of polyolefins over acidic catalysts under the fluidized bed reaction. As shown in Figures 2 and 3, it shows that the calculated values using various catalysts are in good agreement with the experimental data. Additionally, in Table III the model gives a good prediction for the correlation coefficient calculated between theoretical and experimental results from the degradation of PP over fluidized cracking catalysts.

### Variation in product generation rates with catalysts

The apparent rate constants based on the model for various catalysts used in this study are also summarized in Table III. The generation of intermediates of long-chain olefins and carbenium ions from the liquid-phase polymer is much faster than other reaction rates such as the generation of (i) the paraffinic lump ($k_{p,c^*}$), (ii) the BTX lump ($k_{a,c^*}$), and (iii) the coke lump ($k_{r,c^*}$). The value of $k_{i,c^*}$ is higher for zeolites (ECat-1 > HZSM-5) than for SAHA. As can be seen in Figure 2, both ECat-1 and HZSM-5 gave more intermediate stream about 70 wt % compared with 60 wt % with SAHA. It seems that zeolites (HZSM-5 and ECat-1) are likely to form a polymer/zeolite complex and consequently to proceed the scission reaction further to generate the volatile products. This also suggests that the nature of the catalyst with zeolites of HZSM-5 and ECat-1 is more effective in converting polymers into

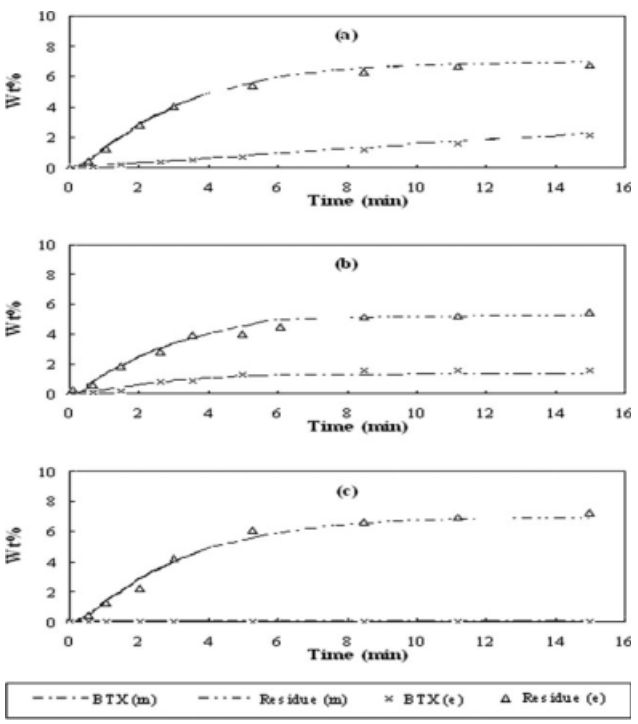


**Figure 3** Comparison of calculated (m) and experimental (e) results of BTX and Residue products for the degradation of PP over (a) HZSM-5, (b) ECat-1 and (c) SAHA catalysts at 360°C (catalyst particle size = 75–120 μm, fluidizing $N_2$ rate = 570 mL $min^{-1}$ and polymer to catalyst ratio = 40% wt/wt).

**TABLE III**
**Comparison of Apparent Rate Constants for the Degradation of PP Over Various Cracking Catalysts at 360°C**

| Catalyst | $k_{i,c^*} \times 10^{-2}$ ($min^{-1}$) | $k_{r,c^*} \times 10^{-2}$ ($min^{-1}$) | $k_{p,c^*} \times 10^{-3}$ ($min^{-1}$) | $k_{a,c^*} \times 10^{-3}$ ($min^{-1}$) | $k_{o,i} \times 10^{-2}$ ($min^{-1}$) | $k_{r,i} \times 10^{-2}$ ($min^{-1}$) | $k_{p,i} \times 10^{-2}$ ($min^{-1}$) | $k_{a,i} \times 10^{-3}$ ($min^{-1}$) | $(R^2)^a$ |
|---|---|---|---|---|---|---|---|---|---|
| HZSM-5 | 254.2 | 1.3 | 1.3 | 0.4 | 29.3 | 0.8 | 10.9 | 9.8 | 0.984 |
| ECat-1 | 231.5 | 2.8 | 7.6 | 0.3 | 16.5 | 2.3 | 25.7 | 6.6 | 0.961 |
| SAHA | 184.7 | 5.1 | 0.6 | <0.1 | 33.5 | 2.1 | 2.7 | <0.1 | 0.987 |

Catalyst particle size = 75–120 μm, fluidizing $N_2$ rate = 570 mL $min^{-1}$ and polymer to catalyst ratio = 40% wt/wt.
[a]The average of a series of correlation coefficients ($k_{o,i}$, $k_{r,i}$, $k_{p,i}$, and $k_{a,i}$, respectively) calculated for the deviations between theoretical and experimental results.

intermediates of volatile precursors than the amorphous SAHA. Acid-catalyzed polymer cracking reactions involve a large number of compounds, reaction and catalyst deactivation and are very complex. Both acidity and diffusion constraints within individual micropores of each catalyst may play significant roles in the product distribution. It can be seen in Figure 2(b) that the calculation of this model for PP degradation over Ecat-1 catalyst gave a higher relevant of olefinic and paraffinic deviation than other catalysts. The systematic experiments and the model discussed in this work indicate that catalyst deactivation is being produced by active-site coverage, and consequently decrease the activity of the catalyst, giving the reason of decreasing of reaction rate with reaction time over the course of the reaction. Since the controlling catalytic parameters will be not only the total number of acid sites but also the number of accessible ones, a fuller model is being developed from the effect on the behavior of catalyst deactivation in related to the structure of catalysts and their acid sites.

In Table III, the order of apparent rate constants of intermediates (long-chain olefins and carbenium ions) and the selectivity of olefins is HZSM-5 > ECat-1 > SAHA, and this is not directly related with the total acidity of the catalysts neither with their acid strength, indicating that there are other factors influencing the catalytic cracking of polymer. As also can be seen in Table III, the order of other rate constants ($k_{r,c^*}$, $k_{p,c^*}$, and $k_{a,c^*}$) associated with the selectivity of each product such as olefins, paraffins, residual and BTX observed is varied with the structure and acidity of catalysts as well as their acid strength. Since the low boiling point reaction products formed by the cracking events occurring at the end of the chain will come out from the reactor, the products with longer chain lengths will stay in the reactor being available for potential recracking processes. It appears that the feed will be cracked at or close to the external surface of the zeolite crystallites and therefore, both acidity and diffusion constraints within individual micropores of each catalyst may play significant roles in the observed product selectivity. Therefore, the subsequent reactions for the generation the olefinic lump, paraffinic lump, BTX lump, and coke lump from long-chain olefins and carbenium ions lump was found to vary with the catalyst used. Higher values of the apparent rate constant of paraffinic lump ($k_{p^*}$) were observed in ECat-1 compared to in HZSM-5 and SAHA, while much higher value of the generation rate of residual lump ($k_{r^*}$) was found in SAHA. For zeolites of HZSM-5 and ECat-1, the generation of olefinic and paraffinic lumps is much faster than the generation of BTX lump and coke lump ($k_{r,i}$). For SAHA, the generation of the olefinic fraction ($k_{o,i}$) is much faster than the other values of the generation of paraffinic lump ($k_{p,i}$) and BTX lump ($k_{a,i}$).

### Product selectivity changes with reacting conditions

In this work, the influence of polymer feed and catalyst type is evaluated. Table IV shows product selectivity of olefins, paraffins, residual and BTX for the competition reactions from intermediate lump (long-chain olefins and carbenium ions). Product selectivity of degradation of both polymers degradation over various catalysts gives similar results on the structurally different polymer feeds. Comparison of zeolites

**TABLE IV**
**Comparison of Product Selectivity for PE and PP Degradation Over Various Catalysts**

| | PE | | | | PP | | | |
|---|---|---|---|---|---|---|---|---|
| Catalyst | $k_{o,i}/k_T^a$ (%) | $k_{r,i}/k_T$ (%) | $k_{p,i}/k_T$ (%) | $k_{a,i}/k_T$ (%) | $k_{o,i}/k_T$ (%) | $k_{r,i}/k_T$ (%) | $k_{p,i}/k_T$ (%) | $k_{a,i}/k_T$ (%) |
| HZSM-5 | 68.7 | 1.8 | 27.2 | 2.3 | 63.9 | 2.2 | 31.3 | 2.6 |
| ECat-1 | 38.5 | 4.8 | 55.3 | 1.4 | 45.2 | 5.6 | 47.6 | 1.6 |
| SAHA | 87.3 | 3.8 | 8.9 | <0.1 | 85.4 | 4.9 | 9.7 | <0.1 |

Catalyst particle size = 75–120 μm, fluidizing $N_2$ rate = 570 mL $min^{-1}$, and polymer to catalyst ratio = 40% wt/wt.
$k_T^a = k_{o,i} + k_{r,i} + k_{p,i} + k_{a,i}$.

**TABLE V**
**Comparison of Product Selectivity for the Degradation of PP Over Different Particle Size of ECat-1 Catalyst in the Temperature Range 290–420°C**

| Temperature (°C) | ECat-1 (75–120 μm) | | | | ECat-1 (125-180 μm) | | | |
|---|---|---|---|---|---|---|---|---|
| | $k_{0,i}/k_T^a$ (%) | $k_{r,i}/k_T$ (%) | $k_{p,\ i}/k_T$ (%) | $k_{a,i}/k_T$ (%) | $k_{0,i}/k_T$ (%) | $k_{r,i}/k_T$ (%) | $k_{p,i}/k_T$ (%) | $k_{a,i}/k_T$ (%) |
| 290 | 46.7 | 5.4 | 46.0 | 1.9 | 43.9 | 6.7 | 46.8 | 2.6 |
| 330 | 42.8 | 5.8 | 49.0 | 1.6 | 41.2 | 5.8 | 50.9 | 2.1 |
| 360 | 38.5 | 4.8 | 55.3 | 1.4 | 36.4 | 5.4 | 56.6 | 1.6 |
| 390 | 34.5 | 3.3 | 61.2 | 1.0 | 33.2 | 4.6 | 61.0 | 1.2 |
| 420 | 36.7 | 3.3 | 59.5 | 0.5 | 39.4 | 3.8 | 56.1 | 0.7 |

Fluidizing $N_2$ rate = 570 mL $min^{-1}$ and polymer to catalyst ratio = 40% wt/wt.
$k_T^a = k_{o,i} + k_{r,i} + k_{p,i} + k_{a,i}$.

in cracking of PE and PP shows an increase in olefinic selectivity with ECat-1 (38.5 vs. 45.2%) and a decrease in paraffinic selectivity with HZSM-5 (27.2 vs. 31.3%). The difference in the amount of olefinic product ($k_{o,\ i}/k_T$) for different catalysts is in the order SAHA (85.4–87.3%) > HZSM-5 (63.9–68.7%) > ECat-1 (38.5–45.2%). Product selectivity varied strongly dependent on catalysts type and structure. The difference in product selectivity for zeolites can be seen with ECat-1 giving a higher selectivity for paraffins and coke than HZSM-5. However, HZSM-5 generates a much higher selectivity for olefins compared with ECat-1. These results may reflect ECat-1 with the combination of pore openings and larger internal supercages allow significant bimolecular reactions and yielded a paraffinic product (47.6–55.3%) and substantial coke levels (4.8–5.6%). The relatively low value (1.8–2.2%) of the $k_{r,i}/k_T$(coke selectivity) suggests that bimolecular reactions such as hydrogen transfer, are sterically hindered within the 10 ring small channel of HZSM-5. The i-butane/n-butane ratio reflects the involvement of tertiary $C_4$ carbenium ions in bimolecular hydrogen transfer reactions and since tertiary carbenium ions are more stable than primary ions, a higher yield of iso-butane would be expected. In our previous study,[31] much higher i-$C_4$/n$C_4$ have been observed in commingled PE/PP/PS cracking for ECat-1 catalyst (with 0.74 nm Y zeolite and silica-alumina bimodal pore structures in the FCC matrix) compared to HZSM-5 (with 0.55 × 0.51 nm narrower pore openings and no supercages), probably because in the absence of the constraints of the ZSM-5 structure the formation bulky bimolecular reaction intermediates is not restricted. Compared with those of zeolites (HZSM-5 and ECat-1), SAHA with large mesopores and low acidity resulted in a relatively low rate of bimolecular reaction to further react to produce paraffins. This also can be seen for zeolites (HZSM-5 = 2.3–2.6%; ECat-1= 1.4–1.6%) produce a much higher selectivity to BTX than for SAHA (<0.1%).

In this model, the rate constants for the catalytic degradation of commingled polymer waste over ECat-1 with particle sizes of 125–180 μm and 75–120 μm at five different temperatures (290–420°C) are also evaluated. Table V shows product selectivity of olefins, paraffins, residual and BTX for the competition reactions from intermediate lump (long-chain olefins and carbenium ions). The selectivity towards the olefinic fraction ($k_{o,i}$) as a function of reaction temperature shows that the amount of olefins formation decreased with increasing reaction temperature from 290 to 390°C then increased at 420°C. On the other hand, the results show the highest amount of paraffinic lump ($k_{p,i}$) occurred at 390°C rather than at the higher temperature of 420°C. It could be the case that selectivity products of paraffins increased with increasing reaction temperature and olefins decreased with an increase in temperature below 390°C. But at higher temperature (420°C), the degradation of commingled polymer waste to volatile products may proceed both by catalytic and thermal reactions leading to the variation of product distributions. Also, the value of coke products ($k_{r,i}/k_T$) increased with temperature as did the values of BTX (aromatic selectivity). Product selectivity of ECat-1 catalyzed degradation of polymer waste gives similar results on both catalyst particle sizes. The external surface of the catalysts is an important factor controlling activity and selectivity. Comparison of zeolites in cracking of PE/PP waste shows an increase in olefinic selectivity with smaller particle ECat-1-S catalyst (75–120 μm) (34.5–46.7% vs. 31.2–43.9%) and a decrease in BTX selectivity (0.5–1.9% vs. 0.9–2.6%) with a lower selectivity for residue (3.3–5.4% vs. 3.8–6.7%) than the larger particle ECat-1-L catalyst (125–180 μm). The result appears that the feed can be cracked at or close to the external surface of the catalysts and therefore, the controlling catalytic parameters will be not only the total number of acid sites but also the number of accessible ones related to the particle size selected.

## Discussion

An important challenge in the process modeling effort is the development of reliable kinetic equations for processes with complex feedstocks. A kinetic/mechanistic model is proposed, and for use to study the

catalytic degradation of polymers and to optimize the potential benefit of catalytic polymer recycling. This model takes into account mechanistic considerations in relation to chemical composition (alkanes, olefins, aromatics, and coke) and catalyst deactivation for the chemical reactions that occurred in the catalytic degradation of polymers. These materials (alkanes, olefins etc.) are present in various molecular weight ranges and, consequently, can be used to define lumps based on the chemical behavior of each group, and to account for chemical reactions. For the mechanism used in this study, the polymer coating the particles is stated to be liquid, and for the reactions that occur on the interior pore surface the situation would seem to be completed. Gaseous products are forced out to have diffused in the macroporos and produced on the interior surface. The kinetic rate constants, representing chemical reactions between lumps, are then no longer purely empirical but they represent the overall kinetics of the possible reactions in the lumped components. Although results over a range of temperatures using a range of catalyst particle sizes has not yet tested to provide information in mass effects, the values of the kinetic constants and the model may be considered as an empirical one. It may be read with moderate interest by some works in polymer pyrolysis.

## CONCLUSION

This article outlines some recent results relevant to the conversion of polymers for the production of potentially valuable hydrocarbons and fuels and also attempts to apply a model for the mechanism and kinetics of catalytic degradation of polymers. A combined kinetic and mechanistic model giving chemical information, applicable to the fluidized-bed reactions, was used to predict production rates and product selectivity for the catalytic degradation of polymers. The model based on a reaction scheme for the observed products and catalyst deactivation in relation to chemistry has been developed. This model gives a good representation of product selectivity and product distributions for catalytic polymer recycling and also provides an improvement of the empirical "lumping" techniques.

## NOMENCLATURE

$C(c)$ coke content, % wt/wt catalyst
$k_{i,j}$ apparent rate constant of the individual reaction of formation of product $i$ from $j$th reaction, $\text{min}^{-1}$
$n_j$ apparent reactor order of $j$th reaction
$r_{i,j}$ rate of the individual reaction of formation of product $i$ from $j$th reaction, g (feed)/g (catalyst) min
$t$ time, min
$W_r$ weight fraction of the individual reaction of reactant $r$ or evolution of product $r$

### Greek letters

$\alpha$ rate of activity loss with coke content, $(\text{wt/wt})^{-1}$
$\eta$ activity of the catalyst
$\eta_j$ activity of the catalyst of the individual $j$th reaction

### Subscripts

$a$ aromatic (BTX) lump
$c^*$ complex of molten polymer/catalyst
$i$ intermediates of olefins and carbenium ions
$o$ olefinic lump
$o^*$ initial acid sites at time $t = 0$
$p$ paraffinic lump
$r$ coke lump
$T$ global apparent rate constant of formation of the olefinic lump, paraffinic lump, BTX lump and coke lump

### References


1. Brandrup, J.; Bittner, M.; Michaeli, W.; Menges, G. Recycling and Recovery of Plastics; Carl Hanser Verlag: Munich, New York, 1996.
2. Lee, M. Chem Britain 1995, 31, 515.
3. Kagayama, M.; Igarashi, M.; Fukada, J.; Kunii, D. Thermal Conversion of Solid Wastes and Biomass. ACS Symposium Series: Washington DC 1980; Vol. 130, p 527.
4. Igarashi, M.; Hayafune, Y.; Sugamiya, R.; Nakagawa, Y. J Energy Resour Technol 1984, 106 377.
5. Hardman, S.; Leng, S. A.; Wilson, D. C. (BP Chemicals Ltd, Polymer Cracking). Eur. Pat. Appl 567292, 1993.
6. Kaminsky, W.; Schlesselmann, B.; Simon, C. J Anal Appl Pyrol 1995, 32, 19.
7. Sodero, S. F.; Berruti, F.; Behie, L. A. Chem Eng Sci 1996, 51, 2805.
8. Uemichi, Y.; Kashiwaya, Y.; Tsukidate, M.; Ayame, A.; Kanoh, H. Bull Chem Soc Jpn 1983, 56, 2768.
9. Vasile, C.; Onu, P.; Barboiu, V.; Sabliovshi, M.; Ganju, D.; Florea, M. Acta Polym 1985, 36, 543.
10. Ishihara, Y.; Nanbu, H.; Saido, K.; Ikemura, T.; Takesue T. Bull Chem Soc Jpn 1991, 64, 3585.
11. Ohkita, H.; Nishiyama, R.; Tochihara, Y.; Mizushima, T.; Kakuta, N.; Morioka, Y.; Namiki, Y.; Katoh, H.; Sunazyka, H.; Nakayama, R.; Kuroyanagi, T. Ind Eng Chem Res 1993, 32, 3112.
12. Mordi, R. C.; Fields, R.; Dwyer, J. J Anal Appl Pyrol 1994, 29, 45.
13. Garforth, A. A.; Lin, Y.-H.; Sharratt, P. N.; Dwyer, J. Appl Catal A: Gen 1998, 169, 329.
14. Audisio, G.; Bertini, F.; Beltrame, P. L.; Carniti, P. Makromol Chem Macromol Symp 1992, 57, 191.
15. Wu, C.-H.; Chang, C.-Y.; Hor, J.-L.; Shih, S.-M.; Chen, L. W.; Chang, F. W. Waste Management 1993, 13, 221.
16. Lin, Y.-H.; Yang, M.-H. Polym Degrad Stab 2007, 92, 813.

17. Liguras, D. K.; Allen, D. T. Ind Eng Chem Res 1989, 28, 665.
18. Froment, G. F. Chemical Reactions in Complex Mixtures, The Mobil Workshop. Van Nostrand Reinhold: New York, 1991.
19. Feng, W.; Vynckier, E.; Froment, G. F. Ind Eng Chem Res 1993, 32, 2997.
20. Lin, Y.-H.; Yang, M.-H. Energy Fuel 1998, 12, 767.
21. Lin, Y.-H.; Yang, M.-H. J Mol Catal A: Chem 2005, 231, 113.
22. Oliverra, L. L.; Biscaia, E. C. Ind Eng Chem Res 1989, 28, 264.
23. Lin, Y.-H.; Yang, M.-H. J Anal Appl Pyrol 2008, 83, 101.
24. Lin, Y.-H.; Yang, M.-H. Appl Catal B: Environ 2007, 69, 145.
25. Lin, Y.-H.; Yang, M.-H. Appl Catal A: Gen 2007, 328, 132.
26. Lin, Y.-H.; Yang, M.-H. Thermochim Acta 2008, 471, 52.
27. Lin, Y.-H. Experimental and Theoretical Studies on the Catalytic Degradation of Polymers, PhD Thesis, University of Manchester Science and Technology (UMIST), 1998.
28. Kissin, Y. V. J Catal 1996, 163, 50.
29. Dwyer, J.; Rawlence D. J. Catalysis Today 1993, 18, 487.
30. Rigby, A. M.; Kramer, G. T.; van Santen R. A. J Catal 1997, 170, 1.
31. Lin, Y.-H.; Yang, M.-H. Polym Degrad Stab 2009, 94, 25.